

# Benzo[2,1-*c*:3,4-*c'*]bis(1,2,3-thiaselenazole) (BSe) and Its Charge Transfer Chemistry. Crystal and Electronic Structure of [BSe]<sub>3</sub>[ClO<sub>4</sub>]<sub>2</sub>

Leanne Beer,<sup>1a</sup> James F. Britten,<sup>1b</sup> A. Wallace Cordes,<sup>1c</sup> Owen P. Clements,<sup>1a</sup> Richard T. Oakley,<sup>\*,1a</sup> Maren Pink,<sup>1d</sup> and Robert W. Reed<sup>1a</sup>

Department of Chemistry, University of Waterloo, Waterloo, Ontario N2L 3G1, Canada, Department of Chemistry, McMaster University, Hamilton, Ontario L8S 4M1, Canada, Department of Chemistry and Biochemistry, University of Arkansas, Fayetteville, Arkansas 72701, and Department of Chemistry, University of Minnesota, Minneapolis, Minnesota 55455

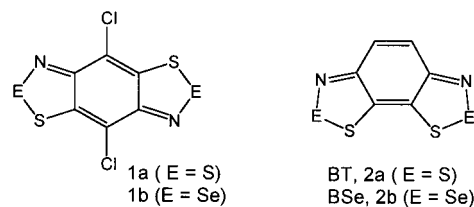
Received April 2, 2001

The S–Se–N-based heterocycle benzo[2,1-*c*:3,4-*c'*]bis(1,2,3-thiaselenazole) (BSe) can be prepared by the condensation of 1,4-diaminobenzene-2,3-dithiol with selenium tetrachloride. Crystals of this compound are not isomorphous with the related benzo[2,1-*c*:3,4-*c'*]bis(1,2,3-dithiazole) (BT); a structure is adopted that allows for more extensive intermolecular Se–Se contacts. Electro-oxidation of BSe in the presence of [*n*-Bu<sub>4</sub>N][ClO<sub>4</sub>] affords metallic green needles of the charge transfer salt [BSe]<sub>3</sub>[ClO<sub>4</sub>]<sub>2</sub>, which exhibit a pressed pellet conductivity  $\sigma(\text{RT}) = 10^{-1} \text{ S cm}^{-1}$ . The crystal structure of [BSe]<sub>3</sub>[ClO<sub>4</sub>]<sub>2</sub> consists of slipped  $\pi$ -stacks based on the triple-decker closed shell [BSe]<sub>3</sub><sup>2+</sup> building block. The packing is analogous to that found for the charge transfer salt [BT]<sub>3</sub>[FSO<sub>3</sub>]<sub>2</sub>, for which  $\sigma(\text{RT}) = 10^{-2} \text{ S cm}^{-1}$ . Extended Hückel band structure calculations on these two (sulfur- and selenium-based) 3:2 salts reveal more extensive intermolecular interactions in the selenium compound. As a result, the latter has a more two-dimensional electronic structure. Crystal data for Se<sub>2</sub>S<sub>2</sub>N<sub>2</sub>C<sub>6</sub>H<sub>2</sub>,  $a = 4.103(2) \text{ \AA}$ ,  $b = 12.159(2) \text{ \AA}$ ,  $c = 16.171(2) \text{ \AA}$ , orthorhombic, *Pbnm*,  $Z = 4$ . Crystal data for Se<sub>6</sub>S<sub>6</sub>N<sub>6</sub>C<sub>18</sub>H<sub>6</sub>Cl<sub>2</sub>O<sub>4</sub>,  $a = 17.00(1) \text{ \AA}$ ,  $b = 18.36(1) \text{ \AA}$ ,  $c = 10.679(4) \text{ \AA}$ , 110.27(3), monoclinic, *C2/c*,  $Z = 4$ .

## Introduction

The early development<sup>2</sup> of the chemistry of 1,2,3-dithiazoles (DTAs) was driven by their potential agricultural applications. More recently, interest has grown in their applications in materials chemistry,<sup>3</sup> in particular as building blocks for both neutral radical<sup>4,5</sup> and radical ion<sup>6–8</sup> based conductors. In this latter regard the benzene-bridged bis(dithiazoles) **1a**<sup>9,10</sup> and **2a** (BT)<sup>11</sup> have been successfully used as templates for the preparation of charge transfer (CT) salts with a variety of stoichiometries and structures. Selenium incorporation into **1a**, to produce the bis(thiaselenazole) **1b**, has also been achieved, but the lack of solubility of this compound precluded any detailed studies of its electrochemistry and charge transfer

chemistry. To explore the effects on charge transfer chemistry of selenium incorporation into a bis(dithiazole), we have prepared the selenium-containing variant benzo[2,1-*c*:3,4-*c'*]bis(1,2,3-thiaselenazole) (**2b**, BSe). While the latter compound also exhibits low solubility in organic media, high-temperature electrocrystallization methods have allowed us to prepare and characterize structurally a perchlorate salt of 3:2 stoichiometry, i.e., [BSe]<sub>3</sub>[ClO<sub>4</sub>]<sub>2</sub>. This represents the first characterization of a CT salt of a thiaselenazole. Here we compare the structural features of BSe, BT, and their CT salts. The results are interpreted in the light of extended Hückel band structure calculations on two isostructural salts of BSe and BT.



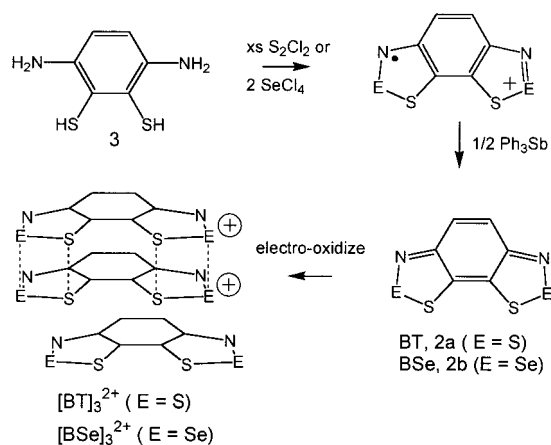
## Results and Discussion

**Synthesis.** The preparative method for BSe (**2b**) follows from that used to generate the sulfur-based compound BT (**2a**) (Scheme 1). Accordingly, when a slurry of the dihydrochloride of diaminobenzene-2,3-dithiol **3** and 2 equiv of SeCl<sub>4</sub> is heated at reflux in dichloroethane for 16 h, a black precipitate of what we presume is the crude radical cation salt [BSe][Cl] is formed.<sup>12</sup> Reduction of the latter with triphenylantimony affords neutral

- (1) (a) University of Waterloo. (b) McMaster University. (c) University of Arkansas. (d) University of Minnesota.
- (2) Kim, K. *Sulfur Rep.* **1998**, *21*, 147.
- (3) (a) Rawson, J. M.; McManus, G. D. *Coord. Chem. Rev.* **1999**, *189*, 135. (b) Torroba, T. *J. Prakt. Chem.* **1999**, *341*, 99.
- (4) Barclay, T. M.; Cordes, A. W.; Haddon, R. C.; Itkis, M. E.; Oakley, R. T.; Reed, R. W.; Zhang, H. *J. Am. Chem. Soc.* **1999**, *121*, 969.
- (5) Barclay, T. M.; Beer, L.; Cordes, A. W.; Oakley, R. T.; Preuss, K. E.; Taylor, N. J.; Reed, R. W. *Chem. Commun.* **1999**, 531.
- (6) Barclay, T. M.; Burgess, I. J.; Cordes, A. W.; Oakley, R. T.; Reed, R. W. *J. Chem. Soc., Chem. Commun.* **1998**, 1939.
- (7) Barclay, T. M.; Cordes, A. W.; Oakley, R. T.; Preuss, K. E.; Reed, R. W. *J. Chem. Soc., Chem. Commun.* **1998**, 1039.
- (8) Barclay, T. M.; Beer, L.; Cordes, A. W.; Haddon, R. C.; Itkis, M. E.; Oakley, R. T.; Preuss, K. E.; Reed, R. W. *J. Am. Chem. Soc.* **1999**, *121*, 6657.
- (9) Barclay, T. M.; Cordes, A. W.; Goddard, J. D.; Mawhinney, R. C.; Oakley, R. T.; Preuss, K. E.; Reed, R. W. *J. Am. Chem. Soc.* **1997**, *119*, 12136.
- (10) Barclay, T. M.; Cordes, A. W.; Mingie, J. R.; Preuss, K. E. *Cryst. Eng. Chem.* **2000**, 15.
- (11) Barclay, T. M.; Cordes, A. W.; Oakley, R. T.; Preuss, K. E.; Reed, R. W. *Chem. Mater.* **1999**, *11*, 164.

- (12) The use of higher boiling solvents, or an excess of SeCl<sub>4</sub>, led to lower overall yields.

## Scheme 1



BSe, which can be purified by crystallization from chlorobenzene followed by fractional sublimation in vacuo.

Attempts to pursue the charge transfer chemistry of **1b** by electrocrystallization methods were thwarted by the insolubility of the compound in organic media. The present compound, BSe (**2b**), suffers from a similar but less acute problem. While the material barely colors chlorinated solvents such as dichloroethane at room temperature, we found that a solubility of ca. 1 mg/50 mL  $\text{C}_2\text{H}_4\text{Cl}_2$  could be induced by heating the solvent to 50–60 °C. At higher temperatures the solubility increased, but we found it difficult (using standard thermostatic baths) to keep such solutions free of turbulence caused by convection currents. With a compromise setting of 55 °C we were able to explore the electro-oxidation chemistry of BSe in the presence of a variety of tetrahedral counterions, including small ( $\text{BF}_4^-$ ), medium ( $\text{ClO}_4^-$  and  $\text{FSO}_3^-$ ), and large ( $\text{FeCl}_4^-$ ,  $\text{GaCl}_4^-$ ) variants. These were introduced to the electrocrystallization cells as 0.1 M solutions of their tetra-*n*-butylammonium salts. Electro-oxidation experiments were performed with a range of current densities, but the best results were obtained using  $\text{ClO}_4^-$  as counterion and a current of 1–2  $\mu\text{A}$ . With this combination, fine, but well-formed metallic green needles of the 3:2 salt  $[\text{BSe}]_3[\text{ClO}_4]_2$  were produced; these were generally harvested after about 5 days. Crystals of  $[\text{BSe}]_3[\text{ClO}_4]_2$  were too small to attempt four- or even two-probe conductivity measurements. Likewise, insufficient quantities were obtained for detailed magnetic measurements. Nonetheless, pressed pellet conductivity measurements provided a value of  $\sigma_{\text{RT}} = 10^{-1} \text{ S cm}^{-1}$ , i.e., the high end of the semiconducting range. We note that this value is 1 order of magnitude higher than those observed for  $[\text{BT}]_3[\text{ClO}_4]_2$  and  $[\text{BT}]_3[\text{FSO}_3]_2$ . The origin of these differences is explored below.

**Crystal Structures.** To provide an internal comparison with the structure of neutral BT and also to establish a benchmark for the internal structural parameters of its CT salt, we have determined the crystal structure of neutral BSe as well as that of  $[\text{BSe}]_3[\text{ClO}_4]_2$ . Crystal data for both compounds are given in Table 1; ORTEP drawings are provided in Figure 1. In contrast to BT, which crystallizes in the monoclinic space group  $P2_1/c$ , crystals of BSe are orthorhombic, space group  $Pbnm$ . In both cases the molecules adopt a slipped  $\pi$ -stack structure, with cell repeat distances along the stack of 3.0033(8) Å (BT) and 4.1031(15) Å (BSe), but the packing of the stacks is significantly different. In BT there are no S–S or S–N intermolecular interactions inside the van der Waals contact,<sup>13</sup> while in BSe there are two

Table 1. Crystal Data

	BSe	$[\text{BSe}]_3[\text{ClO}_4]_2$
formula	$\text{Se}_2\text{S}_2\text{N}_2\text{C}_6\text{H}_2$	$\text{Se}_6\text{S}_6\text{N}_6\text{C}_{18}\text{H}_6\text{Cl}_2\text{O}_4$
fw	324.13	1171.31
<i>a</i> , Å	4.103(2)	17.00(1)
<i>b</i> , Å	12.159(2)	18.36(1)
<i>c</i> , Å	16.171(2)	10.679(4)
$\beta$ , deg	90	110.27(3)
<i>V</i> , Å <sup>3</sup>	806.8(3)	3120(3)
$\rho$ (calcd), g cm <sup>-3</sup>	2.67	2.49
space group	<i>Pbnm</i>	<i>C2/c</i>
<i>Z</i>	4	4
temp, K	293(2)	298(2)
$\mu$ , mm <sup>-1</sup>	9.51	4.06
$\lambda$ , Å	0.71073	0.55942
no. of data/restraints/ params	614/00/55	2611/00/212
solution method	direct methods	direct methods
<i>R</i> , <i>R</i> <sub>w</sub>	0.039, 0.048 (on <i>F</i> ) <sup>a</sup>	0.063, 0.126 (on <i>F</i> ) <sup>b</sup>

<sup>a</sup>  $R = [\sum ||F_o| - |F_c||] / [\sum |F_o|]$ ;  $R_w = \{[\sum w||F_o| - |F_c||^2] / [\sum (w|F_o|^2)]\}^{1/2}$ . <sup>b</sup>  $R = [\sum ||F_o| - |F_c||] / [\sum |F_o|]$ ;  $R_w = \{[\sum w||F_o|^2 - |F_c|^2|^2] / [\sum (w|F_o|^2)]\}^{1/2}$ .

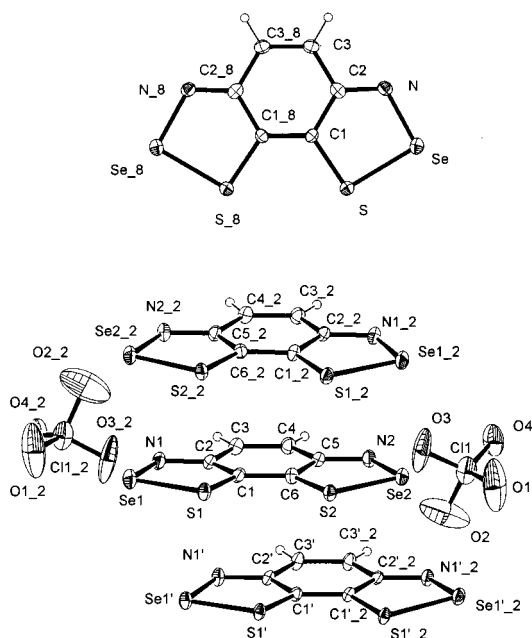


Figure 1. ORTEP drawings (30% probability ellipsoids) showing atom numbering of BSe (above) and  $[\text{BSe}]_3[\text{ClO}_4]_2$  (below).

relatively close Se–S–Se contacts (Figure 2) which lace together the entire molecular array. Mean internal structural parameters are summarized in Table 2, and a listing of pertinent intermolecular Se–S–Se contacts is provided in Table 3.

Given the small size of the crystals, determination of the crystal structure of  $[\text{BSe}]_3[\text{ClO}_4]_2$  was a challenging task, but eventually achieved using synchrotron radiation. The structure of the salt is based upon the triple-decker slipped  $\pi$ -stack  $[\text{BSe}]_3^{2+}$  unit illustrated in Scheme 1. As in the case of the  $[\text{BT}]_3^{2+}$  dication reported earlier, the internal structural features of  $[\text{BSe}]_3^{2+}$  (Table 3) can be described in terms of two layers oxidized to the radical cation level (charge = 1+), while the third layer corresponds to a neutral ring (charge = 0). Thus the S–Se and Se–N distances in the two  $[\text{BSe}]^+$  rings are marginally shorter than those in BSe itself,<sup>14</sup> while those in the (unique) third ring are nearly identical to those in BSe.

(13) Bondi, A. *J. Phys. Chem.* **1964**, *68*, 441.

(14) As expected upon oxidation of an electron from a Se–S and Se–N antibonding orbital.

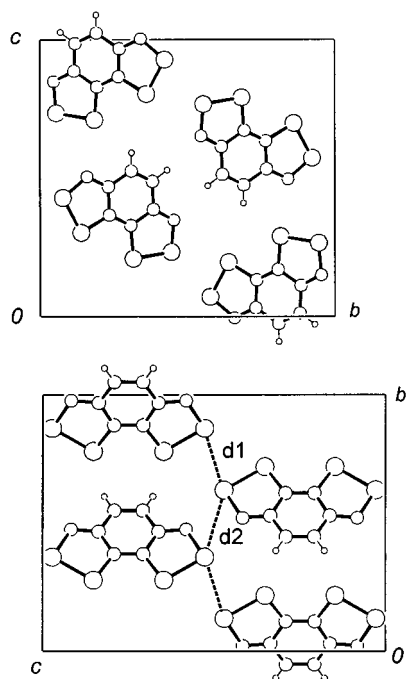


**Figure 2.** Packing of BT (above) and BSe (below), viewed along the  $x$ -direction. Intermolecular Se...Se contacts in BSe are defined in Table 3.

**Table 2.** Summary of Mean Intramolecular Distances ( $\text{\AA}$ )<sup>a</sup>

formal charge	BSe	[BSe] <sub>3</sub> [ClO <sub>4</sub> ] <sub>2</sub>	
	BSe	[BSe] <sub>2</sub> <sup>2+</sup>	BSe
S-Se	2.259(1)	2.23(1)	2.264(2)
Se-N	1.819(4)	1.77(1)	1.798(6)
S-C	1.751(5)	1.72(1)	1.745(7)
N-C	1.306(6)	1.33(1)	1.321(8)
(S)C-C(S)	1.35(1)	1.409(9)	1.39(1)

<sup>a</sup> The numbers in parentheses are the greater of the range and the standard deviation.

**Table 3.** Intermolecular contacts ( $\text{\AA}$ ) in BSe and [BSe]<sub>3</sub>[ClO<sub>4</sub>]<sub>2</sub>

contact	BSe		contact	[BSe] <sub>3</sub> [ClO <sub>4</sub> ] <sub>2</sub>	
	d1	3.681(1)		d2	3.683(1)
d3 (Se1...Se1)	3.415(1)	d4 (S2...S1)	3.363(2)		
d5 (Se1...Se1)	3.806(1)	d6 (S1...S1')	3.702(2)		
d7 (Se1'...Se2)	3.669(1)	d8 (S1'...S2)	3.758(2)		
d9 (Se1...Se2)	3.648(1)				
d10 (Se1'...Se1')	3.707(1)				

Inspection of the intramolecular contacts in the dimeric (BSe)<sub>2</sub><sup>2+</sup> unit reveals Se...Se and S...S separations that are marginally longer than those found in the loosely associated triple-decker cations **4** and **5**.<sup>15</sup>

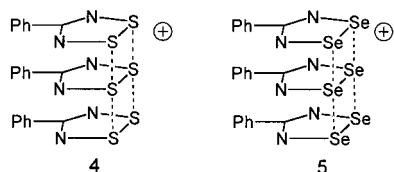


**Figure 3.** Packing of [BSe]<sub>3</sub>[ClO<sub>4</sub>]<sub>2</sub>, viewed down the  $z$  direction.

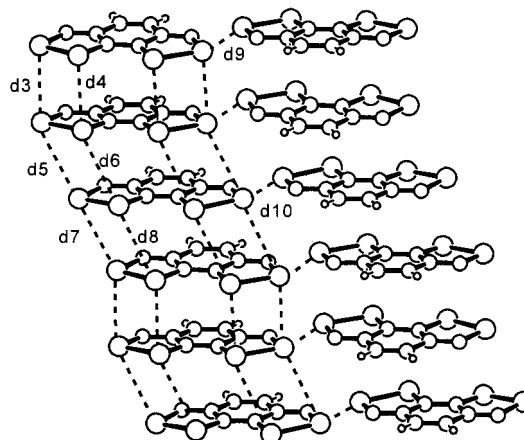


**Figure 4.** Stacking of [BSe]<sub>3</sub><sup>2+</sup> units in [BSe]<sub>3</sub>[ClO<sub>4</sub>]<sub>2</sub>. The anions have been omitted for purposes of clarity. Se...Se and S...S contacts are defined in Table 3.

structures contain a triple-decker [BT]<sub>3</sub><sup>2+</sup> unit, analogous to the [BSe]<sub>3</sub><sup>2+</sup> described here, the packing of the [BT]<sub>3</sub><sup>2+</sup> units is quite different. Of the two structures, that of [BT]<sub>3</sub>[FSO<sub>3</sub>]<sub>2</sub> is essentially the same as that of [BSe]<sub>3</sub>[ClO<sub>4</sub>]<sub>2</sub>; there are minor variations in the positions and orientations of the anions, but the arrangement of the triple-decker dications is virtually identical. Both compounds belong to the same space group  $C2/c$ , and the crystallographic building block is actually one-half of the chemical building block. The neutral BSe/BT molecule is bisected by a 2-fold rotation axis. As a result, the asymmetric unit consists of half of the neutral molecule and one radical cation molecule. In both compounds the triple-decker units align themselves into what resembles snakelike arrays along the  $x$  direction (Figure 3); these layers are interspersed by anions (FSO<sub>3</sub><sup>-</sup> for BT and ClO<sub>4</sub><sup>-</sup> for BSe).

When viewed from a direction approximately parallel to  $y$  (Figure 4), the slipped  $\pi$ -stack arrangement of the triple-decker dications becomes apparent. Both [BT]<sub>3</sub>[FSO<sub>3</sub>]<sub>2</sub> and [BSe]<sub>3</sub>[ClO<sub>4</sub>]<sub>2</sub> exhibit the same number and kind of intermolecular contacts along the stacks. However, while [BT]<sub>3</sub>[FSO<sub>3</sub>]<sub>2</sub> shows no close intermolecular (S...S) contacts, [BSe]<sub>3</sub>[ClO<sub>4</sub>]<sub>2</sub> displays a network of lateral intermolecular Se...Se interactions (contacts d9 and d10) which fall within the van der Waals separation (3.8  $\text{\AA}$ );<sup>13</sup> the effect of these on the band structure of the compound is described below.

**Electronic Structure Calculations.** Given the similarity in the structures of [BSe]<sub>3</sub>[ClO<sub>4</sub>]<sub>2</sub> and [BT]<sub>3</sub>[FSO<sub>3</sub>]<sub>2</sub>, we wished to explore the electronic effects of the replacement of sulfur by selenium within an essentially isostructural environment. To

In the case of BT, two different 3:2 salts, with FSO<sub>3</sub><sup>-</sup> and ClO<sub>4</sub><sup>-</sup> anions, have been characterized.<sup>11</sup> While both these

(15) Bryan, C. D.; Cordes, A. W.; Haddon, R. C.; Hicks, R. G.; Oakley, R. T.; Palstra, T. T. M.; Perel, A. M.; Scott, S. R. *Chem. Mater.* **1994**, *6*, 508.

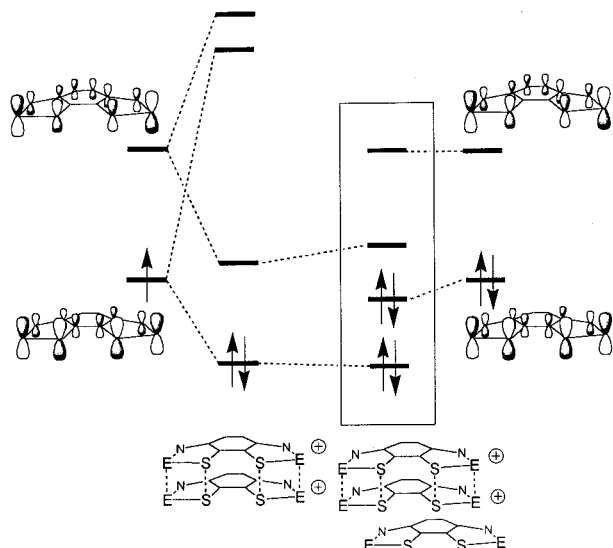


**Figure 5.** FMO diagram illustrating the evolution of the electronic structure of one  $[\text{BSe}]_3^{2+}$  or  $[\text{BT}]_3^{2+}$  unit starting from two radical cations and a neutral molecule (E = S or Se).

what extent does the presence of selenium increase intermolecular interactions, and how are bandwidths and band gaps affected? To address these points, we have carried out a series of extended Hückel molecular and band electronic structure calculations. The results are conveniently described with the aid of a frontier molecular orbital (FMO) diagram (Figure 5), which monitors the frontier orbital changes that accompany the assembly of a single triple-decker  $[\text{BSe}]_3^{2+}$  or  $[\text{BT}]_3^{2+}$  unit from its constituents, i.e., two radical cations and one closed shell molecule. We have used similar arguments in the past to account for the differences (molecular and solid state) in the electronic structures of species such **4** and **5**.<sup>15</sup>

As a first step in this process, one can envisage the dimerization of two radical cations into the corresponding  $[\text{BSe}]_2^{2+}$  or  $[\text{BT}]_2^{2+}$  species. These dimers are closed shell, although the LUMOs, i.e., the in-phase combination of the (SOMO+1)s of the two radical cations, are relatively low lying. Introduction of a third, but laterally displaced, closed shell molecule leads to more limited interactions, the most important of which is between the HOMO of the neutral ring and the LUMO of the dimeric dication. In the case of  $[\text{BT}]_3^{2+}$ , the perturbation of the incoming energies is relatively slight, as the interannular S--S and S--N contacts are long. However, in  $[\text{BSe}]_3^{2+}$ , the presence of selenium rather than sulfur leads to stronger orbital mixing, so that the HOMO of  $[\text{BSe}]_3^{2+}$  is lowered and the LUMO raised, relative to the corresponding orbitals in  $[\text{BT}]_3^{2+}$ . The net result is that the HOMO–LUMO gap in  $[\text{BSe}]_3^{2+}$  is, at the molecular level, larger than that in  $[\text{BT}]_3^{2+}$  (0.30 vs 0.11 eV at the EHMO level). Insofar as the higher conductivity of  $[\text{BSe}]_3[\text{ClO}_4]_2$  compared to that of  $[\text{BT}]_3[\text{FSO}_3]_2$  can be related to band gap differences, these molecular electronic effects are, at first view, surprising.

A full explanation requires consideration of solid state interactions. Given the layerlike structures of  $[\text{BSe}]_3[\text{ClO}_4]_2$  and  $[\text{BT}]_3[\text{FSO}_3]_2$ , i.e., slipped  $\pi$ -stack arrays of triple-decker dications interspersed by anions, we have chosen to restrict our analysis of the electronic structures of these solids to a two-dimensional model consisting of a single layer of dications lying in a plane perpendicular to  $y$ ; the very small effect of interactions across the anionic layers has been neglected. The results, plotted as the crystal orbital dispersion curves arising from the four molecular frontier orbitals highlighted in Figure 4, are shown

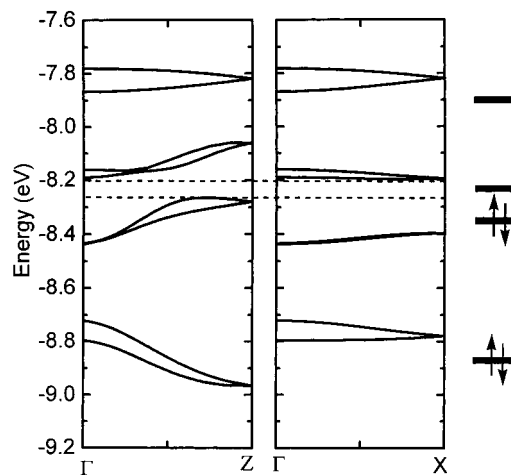


**Figure 6.** Two-dimensional band structure of  $[\text{BT}]_3[\text{FSO}_3]_2$ , showing dispersion curves for the four orbitals highlighted in Figure 5. Orbital energies of a single  $[\text{BT}]_3^{2+}$  dication are shown on the right. The band gap region is indicated with dashed lines.

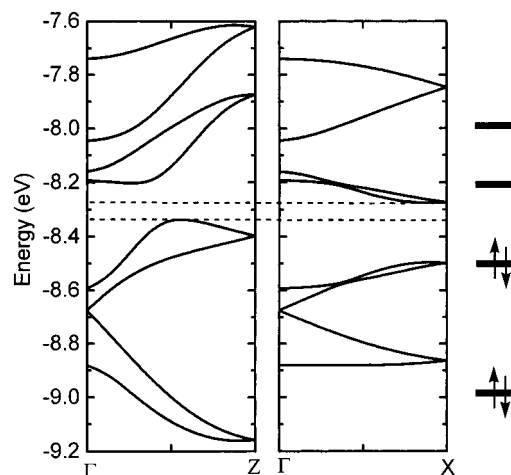


**Figure 7.** Two-dimensional band structure of  $[\text{BSe}]_3[\text{FSO}_3]_2$ , showing dispersion curves for the four orbitals highlighted in Figure 5. Orbital energies of a single  $[\text{BSe}]_3^{2+}$  dication are shown on the right. The band gap region is indicated with dashed lines.

in Figures 6 and 7. The curves track the wavevector  $k$  along the  $c^*$  and  $a^*$  directions in reciprocal space, and while these directions do not correspond exactly to real space directions, they can be loosely related, respectively, to orbital interactions along and across the molecular  $\pi$ -stacks. In the  $[\text{BT}]_3^{2+}$  system dispersion of the HOMO along  $c^*$  leads to some diminution of the band gap, but changes in the LUMO are small: indeed the dispersion curve along  $a^*$  is almost flat. The net effect of these lateral interactions is to reduce the indirect band gap from 0.11 to 0.06 eV. In the  $[\text{BSe}]_3^{2+}$  structure orbital dispersion is more pronounced, as a result of the more extensive overlap properties of selenium. Dispersion is enhanced not only along the stacking direction, but also lateral to it; collectively and individually the effects are significantly larger than those observed in organic materials.<sup>16</sup> The HOMO is raised substantially, as before, but now the LUMO is also dispersed by interactions between the stacks, i.e., the structure is more two-dimensional.<sup>17</sup> As a result, the band gap is reduced from 0.30 to 0.06 eV, the same value as that found for  $[\text{BT}]_3^{2+}$ .

(16) Cornil, J.; Calbert, J. Ph.; Bréda, J. L. *J. Am. Chem. Soc.* **2001**, *123*, 1250.

(17) Cordes, A. W.; Haddon, R. C.; Hicks, R. G.; Oakley, R. T.; Vajda, K. E. *Can. J. Chem.* **1998**, *76*, 307.

## Summary and Conclusions

Electro-oxidation of closed shell bis(1,2,3-dithiazoles) leads to a rich array of conductive charge transfer salts. In this work we have extended the exploration of these systems to selenium-containing variants. Selenium incorporation leads to a severe reduction in solubility of the neutral materials, but in this case the problem could be surmounted, and we were able to characterize structurally the first charge transfer salt of a bis-(thiaselenazole). The crystal structure of  $[\text{BSe}]_3[\text{ClO}_4]_2$  is isostructural with that of  $[\text{BT}]_3[\text{FSO}_3]_2$ , and extended Hückel band structure calculations on the two slipped  $\pi$ -stack structures reveal the importance of both intra- and interstack interactions in the selenium-based compound in reducing the band gap. Both compounds are predicted, at this level of theory, to be small band gap semiconductors, in agreement with their respective room-temperature conductivities. In general terms the magnitude of the lateral interactions in the  $[\text{BSe}]_3[\text{ClO}_4]_2$  is encouraging and augurs well for the pursuit of conductive materials, both neutral and charged, based on bis(thiaselenazole) frameworks.

## Experimental Section

**General Procedures and Starting Materials.** Elemental selenium, *p*-phenylenediamine, and triphenylantimony were obtained commercially (Aldrich). Chlorine gas (Matheson) was used as received. The electrolytes  $[n\text{-Bu}_4\text{N}][\text{X}]$ , with  $\text{X}^- = \text{BF}_4^-, \text{PF}_6^-, \text{and } \text{ClO}_4^-$ , were also obtained commercially (Fluka) and used as received, while for  $\text{X}^- = \text{GaCl}_4^-$  and  $\text{FSO}_3^-$  the materials were prepared and purified according to literature procedures.<sup>18</sup> Diaminobenzenedithiol **3** (as its dihydrochloride)<sup>19</sup> and selenium tetrachloride<sup>20</sup> were also prepared according to standard literature methods. The solvents chlorobenzene (Fisher), dichloroethane (Fisher), and acetonitrile (Fisher HPLC grade) were commercial products and dried by distillation from  $\text{P}_2\text{O}_5$ . All reactions were carried out under an atmosphere of nitrogen. Fractional sublimations were performed in an ATS series 3210 three-zone tube furnace, mounted horizontally, and linked to a series 1400 temperature control system. Melting points are uncorrected. Elemental analyses were performed by MHW Laboratories, Phoenix, AZ. Infrared spectra were recorded (at  $2\text{ cm}^{-1}$  resolution on Nujol mulls) on a Nicolet Avatar FTIR spectrometer.

**Preparation of BSe (2b).** A slurry of diaminobenzenedithiol dihydrochloride **3** (1.1 g, 4.44 mmol) and  $\text{SeCl}_4$  (2.2 g, 9.97 mmol) in 60 mL of dichloroethane was heated at reflux for 24 h. The resultant insoluble black solid was filtered off, washed with  $2 \times 10\text{ mL}$  of  $\text{CH}_3\text{CN}$ , and dried in vacuo. This solid, crude  $[\text{BSe}][\text{Cl}]$ , was reduced by heating it with triphenylantimony (2.5 g, 7.08 mmol) in 60 mL of  $\text{CH}_3\text{CN}$  for 6 h. The black product was filtered off, washed with  $2 \times 10\text{ mL}$  of  $\text{CH}_3\text{CN}$ , and dried in vacuo. This material was purified by recrystallization from 800 mL of chlorobenzene to afford BSe as a brown/black granular solid (1.0 g). Further purification was effected by slow (10 days) fractional sublimation from 160 to  $110\text{ }^\circ\text{C}/10^{-2}\text{ Torr}$  to afford metallic bronze needles. Overall yield of sublimed material: 0.20 g, 0.632 mmol, 13%, dec  $> 250\text{ }^\circ\text{C}$ . Anal. Calcd for  $\text{C}_6\text{H}_2\text{N}_2\text{S}_2\text{Se}_2$ : C, 22.23; H, 0.62; N, 8.62. Found: C, 22.43; H, 0.51; 8.67. IR ( $1600\text{--}400\text{ cm}^{-1}$ ): 1513 (w), 1489 (w), 1435 (w), 1406 (m), 1301 (vs), 1332 (m), 1068 (s), 904 (w), 815 (vs), 747 (m), 696 (vs), 559 (w), 462 (s)  $\text{cm}^{-1}$ .

(18) (a) Taylor, M. J.; Tuck, D. G. *Inorg. Synth.* **1983**, 22, 135. (b) Cox, D. D.; Ball, G. A.; Alonso, A. S.; Williams, J. M. *Inorg. Synth.* **1989**, 26, 393.

(19) (a) Green, A. G.; Perkin, A. G. *J. Chem. Soc.* **1903**, 83, 1201. (b) Lakshmikantham, M. V.; Raasch, M. S.; Cava, M. P.; Bott, S. G.; Atwood, J. L. *J. Org. Chem.* **1987**, 52, 1874.

(20) Brauer, G. *Handbook of Preparative Inorganic Chemistry*; Academic Press: New York, 1963; Vol. 1, p 243.

**Electrocrystallizations.** The electrocrystallization work employed a variation of standard H-cell techniques.<sup>21</sup> A 500 mL round-bottom cell fitted with a sidearm was used as the electrochemical cell, with the Pt wire working electrode (anode) introduced through the main neck. The Pt wire cathode (counter-electrode) was inserted through the sidearm, which was separated from the bulk solution by a porous glass (D) frit. Samples of BSe (10 mg) were dissolved (over a 24 h period) in 500 mL of  $\text{C}_2\text{H}_4\text{Cl}_2$  containing 0.02–0.2 M  $[n\text{-Bu}_4\text{N}][\text{X}]$  ( $\text{X} = \text{BF}_4^-, \text{GaCl}_4^-, \text{FSO}_3^-, \text{ClO}_4^-, \text{PF}_6^-$ ) at  $55\text{ }^\circ\text{C}$ . The cells were then immersed in a VWR 1225 PC water bath containing ethylene glycol, which was thermostatically maintained at  $55\text{ }^\circ\text{C}$  ( $\pm 1\text{ }^\circ\text{C}$ ). Currents ranged from 1 to  $2.0\text{ }\mu\text{A}$ , with growth periods of 5–7 days. Well-formed but very small green metallic crystals were prepared consistently with  $\text{ClO}_4^-$  as counterion; the material is stable in air.

**X-ray Measurements.** X-ray data on neutral BSe were collected at Arkansas on a CAD-4, ENRAF-Nonius, diffractometer, using Mo  $\text{K}\alpha$  radiation (graphite monochromator) and  $\theta/2\theta$  scans. For  $[\text{BSe}]_3[\text{ClO}_4]_2$  data sets were collected at Arkansas and McMaster. A preliminary structure solution could be obtained, but the crystals were too small and the data sets too weak to provide a quality refinement. Therefore, data sets were collected at NSLS, Brookhaven National Laboratory, and at APS, Argonne National Laboratory, on a Kappa SMART system, Bruker, equipped with a two-by-two array of 1K CCD detectors ( $\lambda = 0.55942\text{ \AA}$ , diamond [111] monochromator) using  $\phi$ -scans. The latter measurements were conducted during commissioning time of beamline 15C at ChemMat CARS. All data were corrected for absorption.<sup>22</sup> Both structures were solved using direct methods and refined using full-matrix least squares.<sup>23</sup> All non-hydrogen atoms were refined with anisotropic displacement parameters. All hydrogen atoms were placed in ideal positions and refined as riding atoms with individual isotropic displacement parameters. Details are provided in Table 1.

**Electronic Structure Calculations.** Molecular and band electronic structure calculations were performed with the EHMACC suite of programs<sup>24</sup> using the parameters discussed previously.<sup>25</sup> The off-diagonal elements of the Hamiltonian matrix were calculated with the standard weighting formula.<sup>26</sup> Atomic positions were taken from X-ray data.

**Acknowledgment.** We thank the Natural Science and Engineering Research Council of Canada and the State of Arkansas for financial support. We also thank the Arkansas Science and Technology Authority for support of the X-ray facilities (at Arkansas) and acknowledge P. Coppens (NSLS) and J. Viccaro (APS) for assistance at the beamline and cooperation.

**Supporting Information Available:** An X-ray crystallographic file in CIF format. This material is available free of charge via the Internet at <http://pubs.acs.org>.

IC010357J

(21) (a) Ferraro, J. R.; Williams, J. M. In *Introduction to Synthetic Electrical Conductors*; Academic Press: New York, 1987; p 25. (b) Stephens, D. A.; Rehan, A. E.; Compton, S. J.; Barkhau, R. A.; Williams, J. M. *Inorg. Synth.* **1986**, 24, 135.

(22) An empirical correction for absorption anisotropy: Blessing, R. *Acta Crystallogr.* **1995**, A51, 33.

(23) The BSe structure was solved and refined using NRC386, a PC version of NRCVAX. Gabe, E. J.; Lepage, Y.; Charland, J. P.; Lee, F. L.; White, P. S. *J. Appl. Crystallogr.* **1989**, 22, 383. The  $[\text{BSe}]_3[\text{ClO}_4]_2$  structure was solved and refined with SHELXTL-Plus V5.10, Bruker Analytical X-ray Systems, Madison, WI.

(24) EHMACC, Quantum Chemistry Program Exchange, program number 571.

(25) (a) Cordes, A. W.; Haddon, R. C.; Oakley, R. T.; Schneemeyer, L. F.; Waszczak, J. V.; Young, K. M.; Zimmerman, N. M. *J. Am. Chem. Soc.* **1991**, 113, 582. (b) Basch, H.; Viste, A.; Gray, H. B. *Theor. Chim. Acta* **1965**, 3, 458.

(26) Ammeter, J. H.; Burghil, H. B.; Thibeault, J. C.; Hoffmann, R. *J. Am. Chem. Soc.* **1978**, 100, 3686.